

Cite this: DOI: 10.1039/c0xx00000x

www.rsc.org/xxxxxx

PAPER

Supplementary information

Cottonised flax fibres vs cotton fibres: structural, textural and adsorption characteristics

Lyuba I. Mikhalovska,^a Vladimir M. Gun'ko,^{a,b} Anna A. Rugal,^b Olena I. Oranska,^b Yuriy I. Gornikov,^b
 5 Claudine Morvan^c Nadège Follain,^c Catherine Domas,^{a,d} Eugene M. Pakhlov^b and Sergey V. Mikhalovsky^{a,*}

Received (in XXX, XXX) Xth XXXXXXXXXX 20XX, Accepted Xth XXXXXXXXXX 20XX

DOI: 10.1039/b000000x

Experimental

10 Methods

Mercury porosimetry

Mercury porosimetry with a PoreMaster (Quantachome Instruments, USA) was used to determine the macropore size distribution of flax fibres (differential PSD $f(D) \sim dV/dD$, Fig. S1, shown for better view as $-dV/d(\log D)$ where D is the pore diameter).

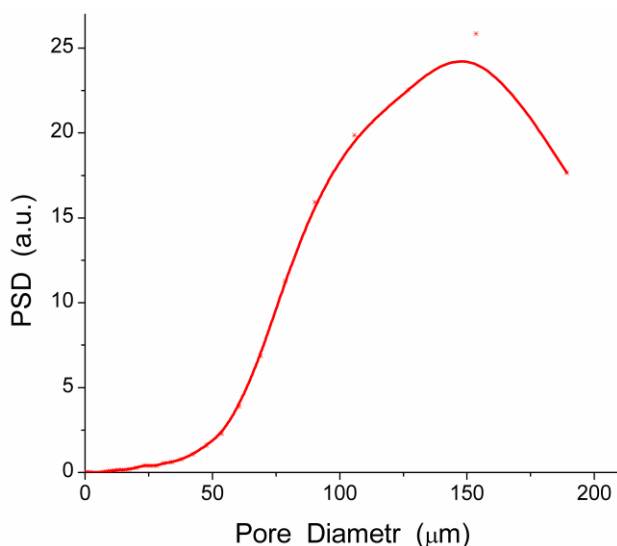


Fig. S1 Macropore size distribution in a bead with flax fibres (mercury intrusion mode).

20 Adsorption of methylene blue (MB)

To calculate the free energy distribution ($f(\Delta G)$) of MB adsorption, the Langmuir equation¹ was used as the kernel of the Fredholm integral equation of the first kind^{2,3}

$$\frac{a}{a_m} = \int \frac{C_{eq} \exp(-\Delta G / R_g T)}{1 + C_{eq} \exp(-\Delta G / R_g T)} f(\Delta G) d(\Delta G) \quad (S1)$$

25 where C_{eq} is the equilibrium MB concentration in a solution, a is the MB adsorption, a_m is the monolayer capacity, and R_g is the gas constant.

The specific surface area was calculated from the MB adsorption isotherms using the area occupied by a MB cation
 30 equal to 1.19 nm² estimated from the adsorption complex (Fig. S2).

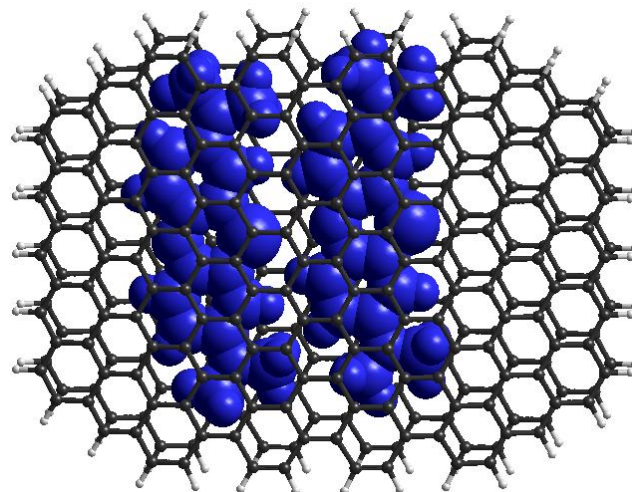


Fig. S2 Adsorption complex of two MB cations in slitshaped nanopore (calculations by CharMM force field with Vega ZZ 2.4.0⁴).

35 Kinetics of MB adsorption onto flax and cotton fibres depends on several processes such as (i) molecular diffusion of MB to a surface and within pores in fibres; (ii) adsorption of individual MB molecules in narrow pores; (iii) adsorption of MB (individual molecules, dimers and oligomers) in broad pores. The MB
 40 adsorption kinetics could be described by the pseudo-first-order (Eq. (S2)) or pseudo-second-order (Eq. (S3)) kinetics

$$\frac{da(t)}{dt} = k_1(a_{eq} - a(t)) \text{ or } \ln(a_{eq} - a(t)) = \ln a_{eq} - k_1 t \quad (S2)$$

$$\frac{da(t)}{dt} = k_2(a_{eq} - a(t))^2 \text{ or } \frac{a(t)}{a_{eq}} = \frac{k_2 a_{eq} t}{1 + k_2 a_{eq} t} \quad (S3)$$

where $a(t)$ is the adsorption (experimental data) as a function of time t , a_{eq} is the equilibrium plateau adsorption, k_1 (in min^{-1}) and k_2 ($\text{dm}^3 \text{min}^{-1} \text{g}^{-1}$) are the adsorption constants. These equations describe saturation effect when MB adsorption reaches a plateau. The second equation in (S3) is a kinetic analogue of the Langmuir adsorption equation.^{1,3}

Natural fibres such as flax and cotton have a complex nonuniform structure. Therefore, the MB adsorption kinetics including several processes mentioned above can be described by overall equation based on Eqs. (S2) and (S3)

$$a(t) = a_{eq} \int_{k_{\min}}^{k_{\max}} \left(w_1(1 - \exp(-kt)) + w_2 \frac{kt a_{eq} / a_0}{1 + kt a_{eq} / a_0} \right) f(k) dk \quad (S4)$$

where w_1 and w_2 are the weight of the pseudo-first-order and pseudo-second-order kinetics, a_0 corresponds to the adsorption of the total amount of dissolved MB, k_{\min} and k_{\max} are the minimal and maximal values of the effective adsorption rate (measured in min^{-1} units) on integration, $f(k)$ is the distribution function of the effective adsorption rate constant.² The $f(k)$ distributions were calculated using a regularisation procedure with unfixed regularisation parameter determined on analysis of experimental data using the F-test and the parsimony principle. Another integral equation describing several types of adsorption kinetics and diffusion can be also used

$$a(t) = \int_{k_{\min}}^{k_{\max}} (w_0 + w_1(1 - \exp(-(kt)^\alpha)) + w_2(1 - \frac{1}{\sqrt{kt}}) + w_3 \ln(1 + kt)) f(k) dk \quad (S5)$$

w_i and α are equation constants. Eq. (S5) describes both non-saturated and saturated adsorption. The k_1 , k_2 , w_i and α constants in Eqs. (S2) – (S5) were calculated using minimisation of the functional

$$\Phi(w_i, k_i, \alpha) = \int_{t_{\min}}^{t_{\max}} \left\{ a_{\text{experimental}}(t) - a_{\text{theoretical}}(t, k_i, w_i, \alpha) \right\}^2 t^{-1} dt \rightarrow \min \quad (S6)$$

where $a_{\text{theoretical}}$ corresponds to Eqs. (S2) and (S3) or the kernels in Eqs. (S4) and (S5). Calculations with all equations were performed for the total time range of the experimental data. For clearness of changes in the $f(k)$ shape over a broad k range (several orders of magnitude), the $f(k)$ distributions were re-calculated into incremental distributions

$$\phi(k_i) = (f(k_{i+1}) + f(k_i)) \times (k_{i+1} - k_i) / 2 \quad (S7)$$

The first moment $\langle x \rangle$ of a distribution function $f(x)$ was calculated with equation

$$\langle x \rangle = \int_{x_{\min}}^{x_{\max}} f(x) x dx / \int_{x_{\min}}^{x_{\max}} f(x) dx \quad (S8)$$

40 Water adsorption

To calculate the free energy distribution ($f(\Delta G)$) of water adsorption, the Langmuir equation was used as the kernel of the Fredholm integral equation of the first kind³

$$\frac{a}{a_m} = \int \frac{p \exp(-\Delta G / R_g T)}{1 + p \exp(-\Delta G / R_g T)} f(\Delta G) d(\Delta G) \quad (S9)$$

where p is the vapour pressure.

Cluster adsorption of water can be described by the equation

$$\frac{a}{a_m} = \frac{bx \left[1 + \sum_{i=2}^m i \varepsilon_i (bx)^{i-1} \right]}{1 + bx \left[1 + \sum_{i=2}^m \varepsilon_i (bx)^{i-1} \right]} \quad (S10)$$

where a_m is the monolayer capacity, $b = z_0 q_1 / (q_0 q_a)$, $z_0 = \exp(\mu_0 / R_g T)$ absolute activity, q_i statistical sum of adsorption complex with i molecules, $\varepsilon_i = \exp(-i(\Delta E_i - \Delta E_0) / R_g T)$, ΔE_i energy of adsorption of the i -th molecule, $x = p / p_s$, m the number of molecules in a cluster at adsorption site. Equation (S10) can be transformed into integral equation

$$\frac{a}{a_m} = \int_{E_{\min}}^{E_{\max}} f(E) \frac{bx \left[1 + \sum_{i=2}^m i \exp(-E / R_g T) (bx)^{i-1} \right]}{1 + bx \left[1 + \sum_{i=2}^m \exp(-E / R_g T) (bx)^{i-1} \right]} dE \quad (S11)$$

where $f(E)$ is the distribution function of adsorption energy of water molecule in adsorbed clusters.³ Eqs. (S9) and (S11) were solved using regularisation procedure² with unfixed regularisation parameter. Eq. (10) was solved using the minimisation of a functional similar Eq. (S6).

The PSD of flax and cotton samples was calculated using water adsorption isotherms with the model of cylindrical pores with the Lennard-Jones parameters for water $\sigma_{ff} = 0.3137 \text{ nm}$, $\varepsilon_{ff} / k_B = 480 \text{ K}$, and water interaction with polymer $\varepsilon_{fs} / k_B = 78.2 \text{ K}$ and $\sigma_{fs} = 0.24 \text{ nm}$ ⁵ using the MND method and the regularisation procedure.^{3,6}

To characterise the adsorption properties of fibres, the adsorption potential (A) distribution ($f(A)$) was calculated as

$$f(A) = -d[\text{spline}(a(p/p_0))] / dA \quad (S12)$$

where a refers to the adsorbed amount of nitrogen or water; and $A = -\Delta G = R_g T \ln(p_0/p)$ and represents the differential molar work equal to the negative change in the Gibbs free energy.⁷ A cubic spline applied to adsorption isotherm $a(p/p_0)$ was used to calculate $f(A)$.

75 TG/DTA measurements

The thermogravimetric (TG) measurements carried out using a Q-1550D (Paulik, Paulik & Erdey, MOM, Budapest) apparatus show that desorption of water (3.7 and 3.9 wt%, respectively, at $T < 150 \text{ }^\circ\text{C}$), depolymerisation and oxidation of organics (300-500 $^\circ\text{C}$) occur in the same temperature ranges for flax and cotton fibres (Fig. S3). The weight loss (TG), differential TG (DTG) and

differential thermal analysis (DTA) curves have similar shapes for them (Fig. S3). Swollen fibres contained approximately 27 wt% of water decomposed at slightly lower temperatures than air-

dry samples (Fig. S3). Ash (mineral residue) was not formed on oxidising of cotton to 700 °C in contrast to flax giving 4.1 wt% of ash.

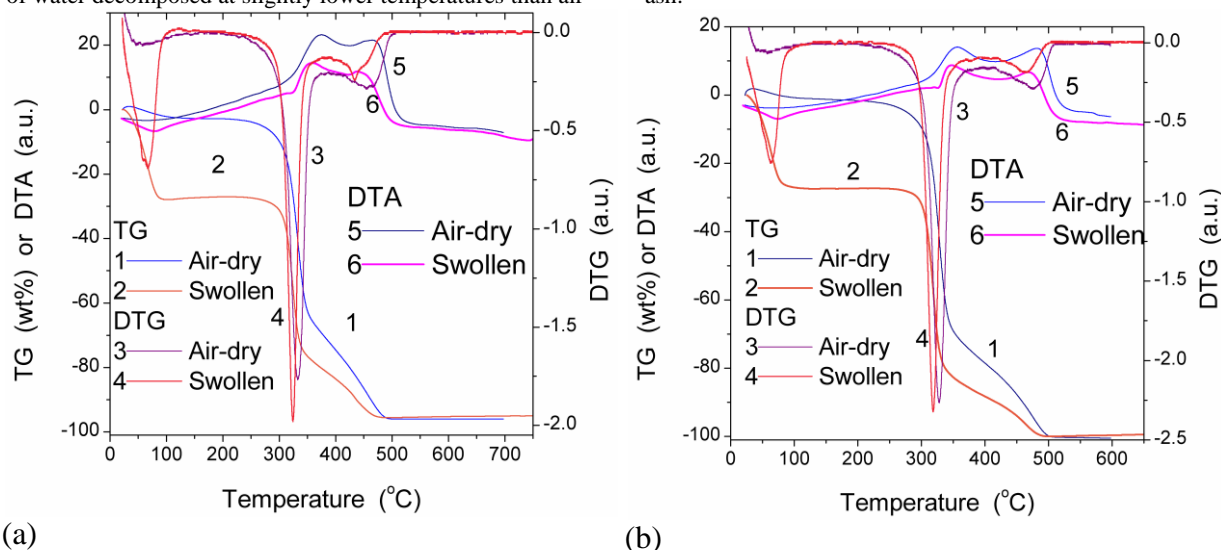


Fig. S3 TG (1, 2), DTG (3, 4) and DTA (5, 6) data for (a) flax and (b) cotton fibres air-dry (1, 3, 5) and swollen for 24 h (2, 4, 6).

XRD

The crystallinity was estimated from integral intensity of XRD

10 patterns (Fig. S4) as described in detail elsewhere.⁸

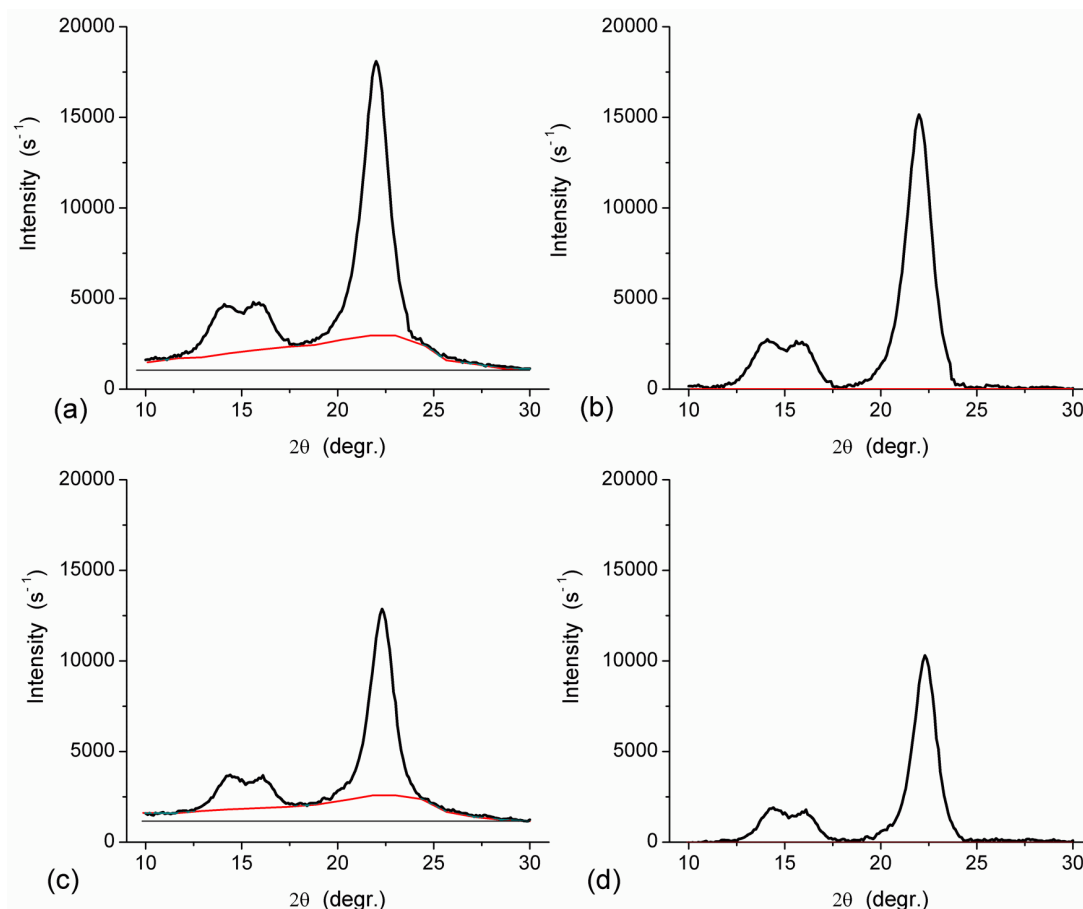
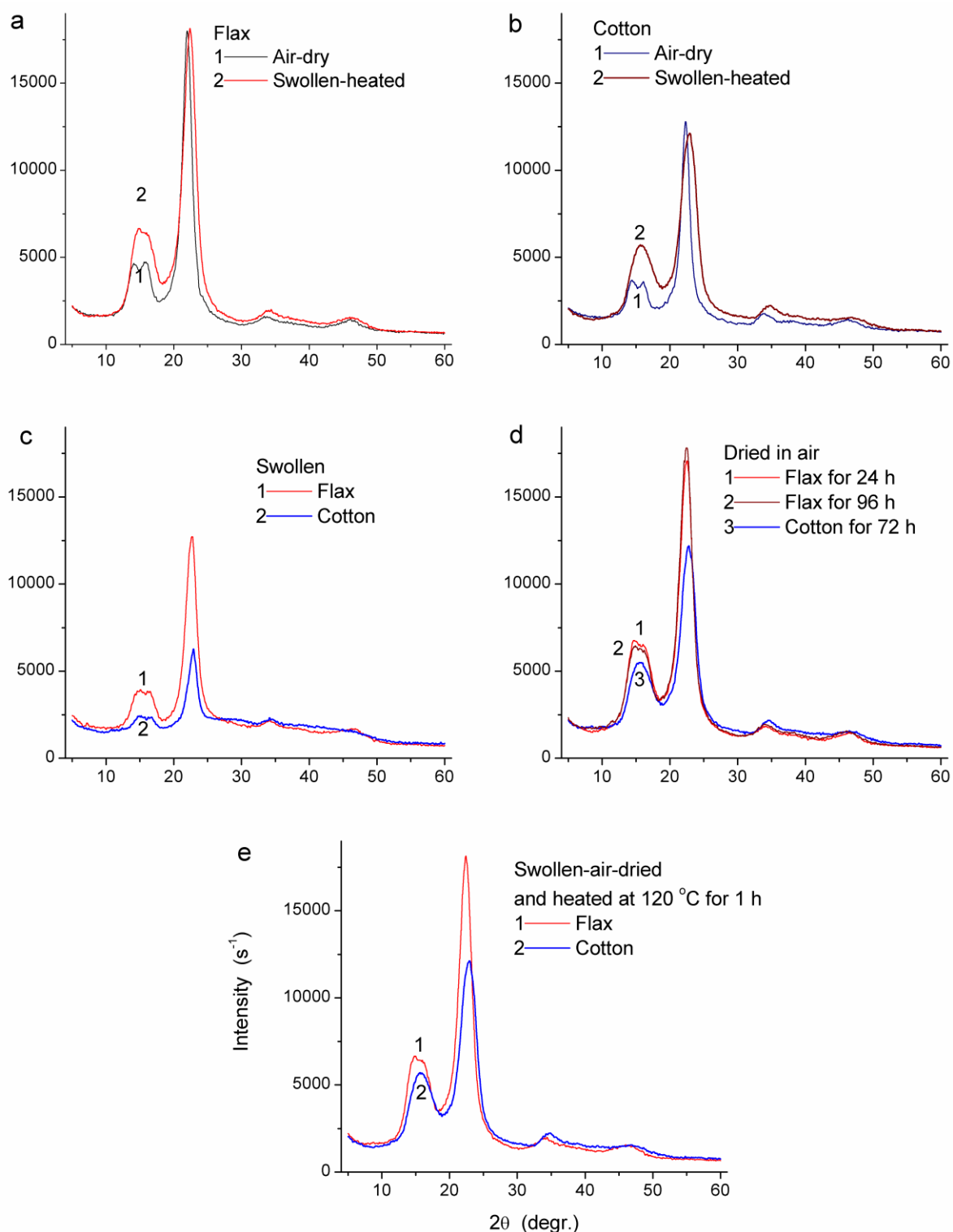


Fig. S4 Determination of crystallinity from integral XRD intensity of crystalline and amorphous fractions of (a, b) flax and (c, d) cotton fibres, (b, d) patterns after subtraction of contribution of amorphous part.

Crystalline structure of fibres changes on swelling (Figs. S5a-c), 15 drying in air (Fig. S5d) and then heating in an oven at 120 °C for

1 h (Fig. S5e). These changes are stronger for cotton than flax. Certain decreases in the size of crystalline structures are observed

(XRD peaks shift towards larger 2θ values) and these changes are greater for cotton fibres.



5 **Fig. S5** XRD patterns of air-dry and 24h swollen fibres: (a) flax, (b) cotton, (c) swollen flax and cotton; (d) swollen fibres dried in air 1-4 days; (e) swollen fibres dried in air and then in oven at 120 °C for 1 h.

In other words, crystallinity of flax is higher and its crystalline structure is more stable than that of cotton fibres.

10

Adsorption of MB and CHX

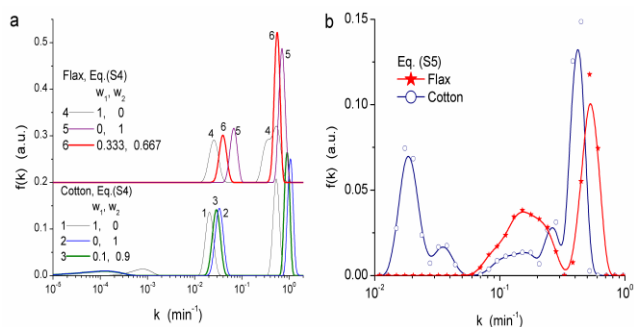


Fig. S6 Distribution functions of MB adsorption rate constant for flax and cotton calculated with integral equations: (a) Eq. (S4) with different weights (w_1 and w_2) of the terms corresponding to pseudo-first and pseudo-second order of adsorption; and (b) Eq. (S5).

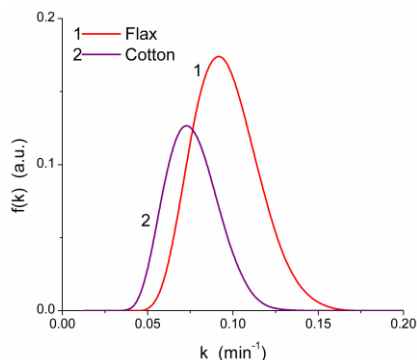


Fig. S7 Distribution functions of CHX adsorption rate constant for flax and cotton calculated with integral equation Eq. (S4) at weights $w_1 = 0.333$ and $w_2 = 0.667$ of the terms corresponding to pseudo-first and pseudo-second order of adsorption.

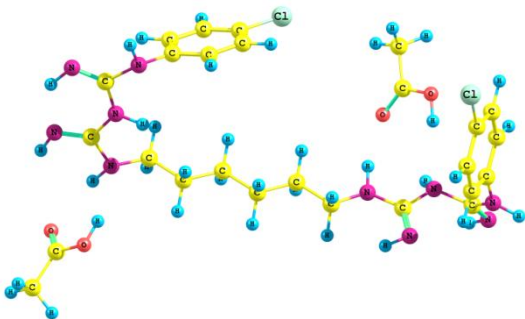


Fig. S8 Chlorhexidine diacetat (6-31G(d,p)⁹ geometry without the hydration effects).

Notes and references

¹⁵ ^a School of Pharmacy & Biomolecular Sciences, University of Brighton, Brighton BN2 4GJ, UK. E-mail: *Tel: 441273 642034; E-mail: s.mikhailovsky@brighton.ac.uk;

^b Chuiko Institute of Surface Chemistry, 17 General Naumov Str., Kiev, Ukraine. Fax: 38044 4243567; Tel: 38044 4229627; E-mail:

²⁰ vlad_gunko@ukr.net;

^c Universite de Rouen/CNRS, UFR des Sciences, 76821 Mon-Saint-Aignan Cedex, France; E-mail: claudine.morvan@univ-rouen.fr

^d University Paul Sabatier, Faculte des Sciences Pharmaceutiques, 118, route de Narbonne, 31062 Toulouse Cedex 9, France; E-mail:

²⁵ catherine.domas@gmail.com

1. A. W. Adamson and A. P. Gast, *Physical Chemistry of Surface*, Sixth edn, Wiley, New York, 1997.

2. S.W. Provencher, *Comput. Phys. Commun.*, 1982, **27**, 213.

- 30 3. V.M. Gun'ko, V.V. Turov and P.P. Gorbik, *Water at the Interfaces*, Naukova Dumka, Kiev, 2009; V.V. Turov, V.M. Gun'ko, *Clustered Water and Ways of Its Applications*, Naukova Dumka, Kiev, 2011; V.M. Gun'ko, *Theor. Experim. Chem.*, 2007, **43**, 139.
4. A. Pedretti, L. Villa and G. Vistoli, *J. Computer-Aided Mol. Design*, 2004, **18**, 167.
- 35 5. O. Vilaseca and L.F. Vega, *Fluid Phase Equilibria*, 2011, **306**, 4; C.E. Ramachandran, S. Chempath, L.J. Broadbelt and R.Q. Snurr, *Micropor. Mesopor. Mat.*, 2006, **90**, 293.
6. V.M. Gun'ko, R. Lebeda, J. Skubiszewska-Zięba, B. Gawdzik and B. Charnas, *Appl. Surf. Sci.*, 2005, **252**, 612.
- 40 7. M. Kruk, M. Jaroniec and K.P. Gadkaree, *Langmuir*, 1999, **15**, 1442.
8. Yu.S. Lipatov, V.V. Shilov, Yu.P. Gomza and N.E. Kruglyak, *Roentgenographic Methods of Study of Polymer Systems*, Naukova Dumka, Kiev, 1982; J.L. Matthews, H.S. Peiser and R.B. Richards, *Acta Cryst.*, 1949, **2**, 85.
- 45 9. M.J. Frisch, G.W. Trucks, H.B. Schlegel, G.E. Scuseria, M.A. Robb, J.R. Cheeseman, J.A. Montgomery, Jr., T. Vreven, K.N. Kudin, J.C. Burant, J.M. Millam, S.S. Iyengar, J. Tomasi, V. Barone, B. Mennucci, M. Cossi, G. Scalmani, N. Rega, G.A. Petersson, H. Nakatsuji, M. Hada, M. Ehara, K. Toyota, R. Fukuda, J. Hasegawa, M. Ishida, T. Nakajima, Y. Honda, O. Kitao, H. Nakai, M. Klene, X. Li, J.E. Knox, H.P. Hratchian, J.B. Cross, V. Bakken, C. Adamo, J. Jaramillo, R. Gomperts, R.E. Stratmann, O. Yazyev, A.J. Austin, R. Cammi, C. Pomelli, J.W. Ochterski, P.Y. Ayala, K. Morokuma, G.A. Voth, P. Salvador, J.J. Dannenberg, V.G. Zakrzewski, S. Dapprich, 50 A.D. Daniels, M.C. Strain, O. Farkas, D.K. Malick, A.D. Rabuck, K. Raghavachari, J.B. Foresman, J.V. Ortiz, Q. Cui, A.G. Baboul, S. Clifford, J. Cioslowski, B.B. Stefanov, G. Liu, A. Liashenko, P. Piskorz, I. Komaromi, R.L. Martin, D.J. Fox, T. Keith, M.A. Al-Laham, C. Y. Peng, A. Nanayakkara, M. Challacombe, P.M.W. Gill, B. Johnson, W. Chen, M.W. Wong, C. Gonzalez, J.A. Pople, *Gaussian 03*, Revision E.01, Gaussian, Inc., Wallingford CT, 2004.